Anisotropic damping of Timoshenko beam elements

Hansen, M.H.

Publication date:
2001

Document Version
Publisher's PDF, also known as Version of record

Risø–R–1267(EN)

Anisotropic damping of Timoshenko beam elements

Morten Hartvig Hansen

Risø National Laboratory, Roskilde, Denmark
May 2001

Abstract This report contains a description of a structural damping model for Timoshenko beam elements used in the aeroelastic code HawC developed at Ris for modeling wind turbines. The model has been developed to enable modeling of turbine blades which often have different damping characteristics for *flapwise*, *edgewise* and *torsional* vibrations. The structural damping forces acting on the beam element are modeled by viscous damping described by an element damping matrix. The composition of this matrix is based on the element mass and stiffness matrices. It is shown how the coefficients for the mass and stiffness contributions can be calibrated to give the desired modal damping in the complete model of a blade.

ISBN 87–550–2881–0; 87–550–2883–7 (Internet)
ISSN 0106–2840

Danka Services International · 2001

Contents

1 Introduction

This report contains a description of a damping model for the Timoshenko beam elements used in the aeroelastic code *HawC*, which is developed at Ris [5] for the modeling of wind turbines.

There are three requirements to a structural damping model for aeroelastic models of wind turbines: It must define the damping forces as *purely dissipative* [6], and it must enable modeling of the *frequency dependency* of structural damping, and the *anisotropic damping characteristics* of moderne wind turbine blades. The first requirement is basic, but it sets an important physical limitation on the modeling of the structural damping forces: They must dissipate energy from *any* vibration of the structure. The second requirement is also basic for structures with internal dissipation in the material.

The third requirement is especially important for wind turbine applications. A LM 19.1 m blade designed with extra high structural damping of its edgewise vibrations is a good example of a blade with anisotropic damping characteristics. Figure 1 shows the logarithmic decrements versus the natural frequencies of this blade obtained from experimental modal analysis. These measurements indicate that the frequency dependency of the modal damping for flapwise, edgewise, and torsional vibrations of the blade is given by three distinct curves.

The anisotropic damping characteristic in Figure 1 cannot be modeled by the traditional Rayleigh damping model which is often used for modeling frequency dependent structural damping. The reason is that the Rayleigh model assumes an isotropic distribution of the viscous damping forces, and can therefore only describe a single curve in the modal damping–frequency diagram. There are methods to construct a viscous damping matrix that can describe *any* desired modal damping–frequency characteristics of a mechanical system (see e.g. [1]). These methods can be used to obtain a HawC model which describes the damping characteristics in Figure 1. However they operate on a global matrix level, and a physical understanding of the damping mechanism based on the global damping matrix is not possible.

Instead a physical damping model for the Timoshenko beam elements is suggested which also enables modeling of the anisotropic damping characteristic in Figure 1. The suggested model is based on viscous damping, and it is introduced by the definition of a damping matrix for the Timoshenko beam element. This

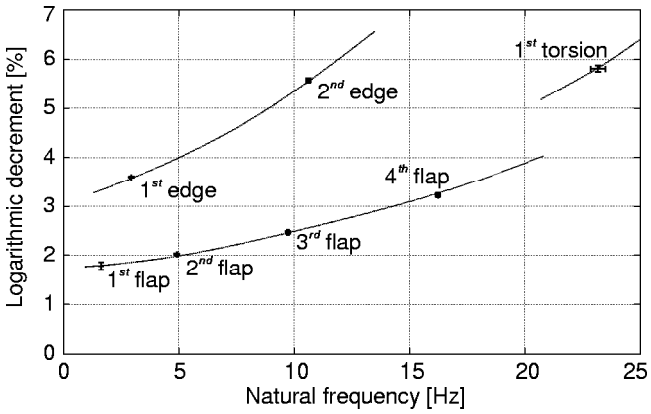

Figure 1. Natural frequencies and logarithmic decrements of the first seven modes for the LM 19.1 m blade (taken from [3]). The points include error bars showing standard deviations of the measurements.

element damping matrix is derived from the element mass and stiffness matrices, but different from Rayleigh damping, the level and frequency dependency of the damping can be set individually for the three principle shapes of vibration: The bending in the two transversal directions and torsion about the axis of the element. Thus, instead of two parameters as for the Rayleigh damping, this suggested model contains six damping parameters.

The report is structured as follows: Section 2 deals with the frequency dependency of viscous damping by studying a single degree of freedom system. The suggested damping model for Timoshenko beam elements is introduced in Section 3. This section also contains an example of damping modeling for the LM 19.1 blade. A conclusion is given in Section 4. Appendix A contains a brief introduction of the Timoshenko beam element. In Appendix B it is shown how the six parameters of the suggested damping model can be calibrated to obtain a particular modal damping of a structure.

2 Viscous damping vs. frequency

In this section a viscous damping model with three different types of damping coefficients is considered: *Mass* and *stiffness proportional* coefficients (similar to Rayleigh damping), and a *mixed mass/stiffness proportional* coefficient. The purpose is to show that viscous damping forces depend on the vibration frequency, and that the frequency dependency changes with the type of damping coefficient. This introductory study forms the basis of choosing two types of damping coefficients used in the viscous damping model for the Timoshenko beam element.

Three different types of viscous damping coefficients

Consider the damped oscillator shown in Figure 2. It has the mass m and the linear spring stiffness k. The viscous damping force of the dash-pot is given by $F_d = -(\eta_m m + \eta_r \sqrt{mk} + \eta_s k)\,\dot{x}$, where the coefficients η_m, η_r, and η_s are the proportionality coefficients of mass, mixed mass/stiffness, and stiffness proportional damping, respectively. Thus, the equation of motion becomes

$$m\ddot{x} + \left(\eta_m m + \eta_r \sqrt{mk} + \eta_s k\right)\dot{x} + kx = 0 \tag{1}$$

where $(\dot{}) \equiv \partial/\partial t$ denotes differentiation with respect to time.

To compute the modal damping of this system, the solution $x = \mathrm{Re}\{x_0 e^{\lambda t}\}$ is inserted into equation (1), and the complex eigenvalue λ is found from the characteristic equation as:

$$\lambda = -\frac{\eta_m}{2} - \frac{\eta_r}{2}\omega - \frac{\eta_s}{2}\omega^2 \pm \sqrt{\left(\frac{\eta_m}{2} + \frac{\eta_r}{2}\omega + \frac{\eta_s}{2}\omega^2\right)^2 - \omega^2} \tag{2}$$

where $\omega \equiv \sqrt{k/m}$ is the undamped angular natural frequency of the oscillator. After substitution of $\lambda \equiv \alpha + i\omega_d$ into the assumed solution, the free oscillations of the damped system are given by $x = e^{\alpha t}\,\mathrm{Re}\{x_0 e^{i\omega_d t}\}$. Hence, the imaginary part of the eigenvalue ω_d is the natural frequency of the damped oscillator, and the real part α is the *damping factor*.

For wind turbine applications the structural damping is low. It can therefore be assumed that $\eta_m + \eta_r\omega + \eta_s\omega^2 << 2\omega$, whereby the squareroot in equation (2) can be approximated by $i\omega$. Thus, the damping factor and natural frequency of the damped oscillator can be approximated by

$$\alpha \approx -\frac{1}{2}\left(\eta_m + \eta_r\,\omega + \eta_s\,\omega^2\right) \qquad \text{and} \qquad \omega_d \approx \omega \tag{3}$$

which show that the mass proportional damping yields a frequency-independent contribution, whereas the contributions due to mixed mass/stiffness and stiffness proportional damping increase with the undamped natural frequency.

As a non-dimensional measure of damping it is possible to use the relative damping exponent $\xi = \alpha/\omega$, or the *logarithmic decrement* $\delta \equiv \log(x(t+T)/x(t))$, where

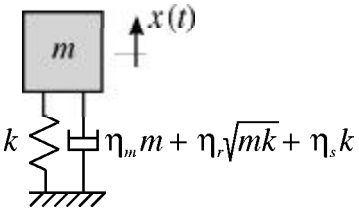

Figure 2. A damped oscillator modeled by the equation of motion (1).

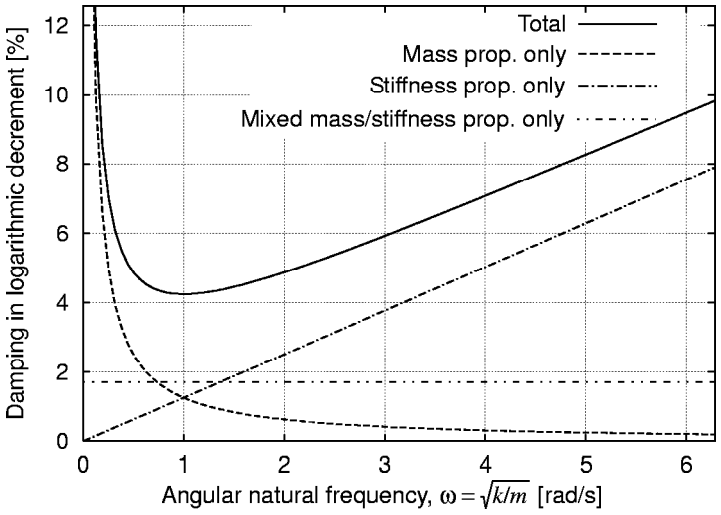

Figure 3. Logarithmic decrement based on equation (4) *for a damped oscillator modeled by the equation of motion* (1).

$T \equiv 2\pi/\omega_d$ is the period of oscillation. The logarithmic decrement (traditionally used at Ris in wind turbine applications) for the damped oscillator is

$$\delta = -\frac{\alpha}{2\pi\omega_d} \approx \frac{1}{4\pi}\left(\eta_m\omega^{-1} + \eta_r + \eta_s\,\omega\right) \tag{4}$$

This equation shows that the logarithmic decrement due to mass proportional damping depend on the frequency as the inverse of the frequency, the mixed mass/stiffness proportional contribution is independent of frequency, and the stiffness proportional contribution increases linear with frequency. These dependencies are illustrated in Figure 3 which shows an example of the logarithmic decrement for the damped oscillator. The individual contributions of mass, mixed mass/stiffness, and stiffness proportional damping are plotted together with the total logarithmic decrement.

Comparison of the damping characteristics in Figure 3 with the measured logarithmic decrements in Figure 1 justify that viscous damping may be used to model the frequency dependency of structural damping of a wind turbine blade. The observed frequency dependency of the logarithmic decrements for flapwise bending modes can be approximated by a curve similar to the total damping curve in Figure 3.

The minimum of the total damping in Figure 3 occurs at $\omega_{\min} = \sqrt{\eta_m/\eta_s}$, and below this frequency the total damping decreases with frequency due to the contribution of mass proportional damping. It may occur that the second flapwise mode is less damped than the first flapwise mode, however such a decrease is often small. The mass proportional damping is therefore assumed unnecessary for the modeling of the frequency dependent damping of wind turbine blades. Only mixed mass/stiffness proportional and stiffness proportional damping are therefore used in the viscous damping model for the Timoshenko beam element suggested in the next section. The first sets the level of damping, and the latter sets the frequency dependency.

3 Damping of Timoshenko beams

In the previous section, it is illustrated that a viscous damping model with mixed mass/stiffness proportional and stiffness proportional damping coefficients can describe the frequency dependency of structural damping.

In this section, it is shown that a combination of this viscous damping model and the Timoshenko beam element enables modeling of the complete anisotropic damping characteristics of wind turbine blades (cf. Figure 1). An element damping matrix is defined for the Timoshenko beam element which describes the distinct damping–frequency dependency of the three principle shapes of blade vibration: Flapwise and edgewise bending vibrations, and torsional vibration. The element damping matrix is shown to be *positive semi-definite* thereby ensuring that the damping forces are purely dissipative, as discussed in the following. The section ends with an example of damping modeling for the LM 19.1 blade.

3.1 Purely dissipative damping

The modeled structural damping forces must dissipate energy from *any* vibration that the structure may undergo. This can be formulated mathematically by requiring that the global damping matrix is positive definite. It can be shown that this requirement is satisfied if the element damping matrix is *positive semi-definite*:

$$\mathbf{u}^T \mathbf{C}_{\text{element}}\, \mathbf{u} \geq 0, \quad \text{for all } \mathbf{u} \in \mathbb{R}^{12} \tag{5}$$

where $\mathbf{u}$ is a displacement vector for the end-nodes of the element (cf. Figure 5 in Appendix A):

$$\mathbf{u} = \{u_{x,1}, u_{y,1}, u_{z,1}, \theta_{x,1}, \theta_{y,1}, \theta_{z,1}, u_{x,2}, u_{y,2}, u_{z,2}, \theta_{x,2}, \theta_{y,2}, \theta_{z,2}\}^T \tag{6}$$

Assuming that the harmonic vibration of the element is given by $\mathbf{x} = \mathbf{u}\sin(\omega t)$, the work of the damping forces over a period of oscillation is given by

$$W_{d,\text{element}} = \int_0^T \dot{\mathbf{x}}^T \mathbf{C}_{\text{element}}\, \dot{\mathbf{x}}\, dt = -\pi\, \omega\, \mathbf{u}^T \mathbf{C}_{\text{element}}\, \mathbf{u} \tag{7}$$

Thus, if the element damping matrix $\mathbf{C}_{\text{element}}$ is positive semi-definite then the work done by the modeled damping forces will be negative, or zero (the case $W_{d,\text{element}} = 0$ can occur for solid body motion of the beam element), showing that they will dissipate energy from any harmonic vibration of the element. This statement can be proven to apply for non-harmonic vibrations as well.

3.2 Mixed mass/stiffness proportional damping

Mixed mass/stiffness proportional damping is used to set the level of damping. Detailed modeling of the damping forces from this type of viscous damping that include coupling of the element DOFs in equation (6), is less important. The mixed mass/stiffness proportional element damping matrix, denoted $\mathbf{C}_{r,\text{element}}$, is therefore chosen to be diagonal, composed only of the diagonal elements of the element mass and stiffness matrices.

Three damping coefficients η_r^x, η_r^y, and η_r^t are introduced to describe the levels damping for flapwise and edgewise bending, and torsion, respectively. Note that in a HawC finite element model of a wind turbine blade, the beam elements are oriented with the x-axis closest to the direction of edgewise bending, and the y-axis closest to the flapwise direction. Thus, the superscripts of the coefficients for flapwise bending η_r^x and edgewise bending η_r^y relate to the axis about which the bending occurs.

With the introduction of the three damping coefficients the 12×12 element matrix for mixed mass/stiffness proportional damping is defined as (for notations and matrices, see Appendix A)

$$\mathbf{C}_{r,\text{element}} = \begin{bmatrix} \mathbf{C}_{r,\text{sub}} & \mathbf{0} \\ \mathbf{0} & \mathbf{C}_{r,\text{sub}} \end{bmatrix} \tag{8}$$

where the 6×6 submatrix $\mathbf{C}_{r,\text{sub}}$ is a diagonal matrix defined as

$$\mathbf{C}_{r,\text{sub}} = \begin{bmatrix} \eta_m^y g_{11} & 0 & 0 & 0 & 0 & 0 \\ 0 & \eta_m^x g_{22} & 0 & 0 & 0 & 0 \\ 0 & 0 & \eta_m^z g_{33} & 0 & 0 & 0 \\ 0 & 0 & 0 & \eta_m^x g_{44} & 0 & 0 \\ 0 & 0 & 0 & 0 & \eta_m^y g_{55} & 0 \\ 0 & 0 & 0 & 0 & 0 & \eta_m^t g_{66} \end{bmatrix} \tag{9}$$

where $g_{ii} \equiv \sqrt{m_{ii} k_{ii}}$, and the coefficient $\eta_m^z \equiv (\eta_m^x + \eta_m^y)/2$ describes the damping of longitudinal vibrations. The choice to compose this damping coefficient as the mean of the coefficients for bending motion is based on the wish to reduce the number of parameters in the model, and the assumption that damping of longitudinal vibrations must be correlated to the damping of both bending motions.

The diagonal elements of $\mathbf{C}_{r,\text{element}}$ are all positive ($g_{ii} > 0$), thus the mixed mass/stiffness proportional damping matrix (8) is positive definite, if all three damping coefficients are positive.

3.3 Stiffness proportional damping

Stiffness proportional damping is used to model the frequency dependency of the structural damping. The physical concept of using stiffness proportional viscous damping is that the internal dissipation due to strain–stress hysteresis is proportional to the rate of change in strain. The linear strains due to flapwise and edgewise bending, and torsion are proportional to the moments of inertia I_x, I_y, and I_z, respectively. The anisotropi of the stiffness proportional damping can therefore be modeled by defining new proportional moments of inertia $\eta_s^x I_x$, $\eta_s^y I_y$, and $\eta_s^t I_z$, where η_s^x, η_s^y, and η_s^t are damping coefficients.

With these moments of inertia, the stiffness proportional element damping matrix becomes (cf. Appendix A)

$$\mathbf{C}_{s,\text{element}} = \begin{bmatrix} \mathbf{C}_{s,11} & \mathbf{C}_{s,12} \\ \mathbf{C}_{s,12}^T & \mathbf{C}_{s,22} \end{bmatrix} \tag{10}$$

where the 6×6 submatrices are defined as

$$\mathbf{C}_{s,11} = \begin{bmatrix} \eta_s^y k_{1\,1} & 0 & 0 & 0 & \eta_s^y k_{1\,5} & \eta_s^y k_{1\,6} \\ \cdots & \eta_s^x k_{2\,2} & 0 & \eta_s^x k_{2\,4} & 0 & \eta_s^x k_{2\,6} \\ \cdots & \cdots & \eta_s^z k_{3\,3} & 0 & 0 & 0 \\ \cdots & sym- & \cdots & \eta_s^x k_{4\,4} & 0 & \eta_s^x k_{4\,6} \\ \cdots & \cdots & metric & \cdots & \eta_s^y k_{5\,5} & \eta_s^y k_{5\,6} \\ \cdots & \cdots & \cdots & \cdots & \cdots & c_{6\,6} \end{bmatrix}$$

$$\mathbf{C}_{s,12} = \begin{bmatrix} -\eta_s^y k_{1\,1} & 0 & 0 & 0 & \eta_s^y k_{1\,5} & -\eta_s^y k_{1\,6} \\ 0 & -\eta_s^x k_{2\,2} & 0 & \eta_s^x k_{2\,4} & 0 & -\eta_s^x k_{2\,6} \\ 0 & 0 & -\eta_s^z k_{3\,3} & 0 & 0 & 0 \\ 0 & -\eta_s^x k_{2\,4} & 0 & \eta_s^x k_{4\,9} & 0 & -\eta_s^x k_{4\,6} \\ -\eta_s^y k_{1\,5} & 0 & 0 & 0 & \eta_s^y k_{5\,10} & -\eta_s^y k_{5\,6} \\ -\eta_s^y k_{1\,6} & -\eta_s^x k_{2\,6} & 0 & \eta_s^x k_{4\,6} & \eta_s^y k_{5\,6} & -c_{6\,6} \end{bmatrix}$$

$$\mathbf{C}_{s,22} = \begin{bmatrix} \eta_s^y k_{1\,1} & 0 & 0 & 0 & -\eta_s^y k_{1\,5} & \eta_s^y k_{1\,6} \\ \cdots & \eta_s^x k_{2\,2} & 0 & -\eta_s^x k_{2\,4} & 0 & \eta_s^x k_{2\,6} \\ \cdots & \cdots & \eta_s^z k_{3\,3} & 0 & 0 & 0 \\ \cdots & sym- & \cdots & \eta_s^x k_{4\,4} & 0 & -\eta_s^x k_{4\,6} \\ \cdots & \cdots & metric & \cdots & \eta_s^y k_{5\,5} & -\eta_s^y k_{5\,6} \\ \cdots & \cdots & \cdots & \cdots & \cdots & c_{6\,6} \end{bmatrix} \tag{11}$$

with

$$c_{6\,6} = \eta_s^t \frac{GI_z}{\ell} + 12\frac{E\left(\eta_s^x I_x e_{s1}^2 \varrho_x + \eta_s^y I_y e_{s2}^2 \varrho_y\right)}{\ell^3}, \tag{12}$$

and the coefficient $\eta_s^z \equiv (\eta_s^x + \eta_s^y)/2$ is used to describe the damping of longitudinal vibrations, as for mixed mass/stiffness proportional damping.

The element damping matrix (10) is positive semi-definite if the three coefficients η_s^x, η_s^y, and η_s^t are positive. This requirement is satisfied because the element stiffness matrix is positive semi-definite for a beam element with any combination of area and moments of inertia.

3.4 Example: The LM 19.1 blade

The suggested damping model is used to model the anisotropic damping characteristics of the LM 19.1 blade (cf. Figure 1). The blade is modeled by a finite element model with 27 nodes using the Timoshenko beam element. The necessary cross-section data for the blade has been supplied by the manufacturer, and few adjustments has been made to obtain agreement between the measured and modeled natural frequencies.

To obtain the six parameters of the damping model $(\eta_r^x, \eta_r^y, \eta_r^t, \eta_s^x, \eta_s^y, \eta_s^t)$, a procedure described in Appendix B is used. The idea of this procedure is to calibrate the damping parameters so that the measured and modeled logarithmic decrements agrees for six lower modes (or when decrements are specified for more than six modes a least squared method is used to minimize the residuals). The six modes that (as a minimum) are chosen for this calibration are the two lowest modes of the three principle shapes of vibration: Flapwise and edgewise bending, and torsion. In the modeling of a wind turbine, the modal logarithmic decrements of its sub-structures are often unknown, however this procedure for calibrating the damping parameters can be used to set a realistic level and frequency dependency of the structural damping.

Figure 4 shows a result for the LM 19.1 blade where the logarithmic decrements of the two lowest flapwise, edgewise, and torsional modes are used to calibrate the damping parameters. Note that the decrement for the second torsional mode has not been measured, so the assumption is made that this mode is damped with the logarithmic decrement of about 14 %.

A comparison of the measured and modeled logarithmic decrements shows that there is an agreement for the six modes used in the calibration. However the measured damping characteristic versus frequency for the four lowest flapwise bending modes has not been captured by the model. A least square method applied to minimize the differences between measured and modeled decrements for all four modes has not improved this result.

There is a possible explanation to why the suggested model does not capture the damping characteristics of the flapwise modes. Flapwise bending is composed of the flapwise translation $u_{y,i}$ and the cross-sectional rotation $\theta_{x,i}$. The stiffness proportional damping of this combined motion is defined by the same damping coefficient η_s^x. For the lower flapwise modes the cross-sectional rotations are small and the damping is dominated by damping of the translational motion. For higher flapwise modes the cross-sectional rotations increase and the stiffness proportional

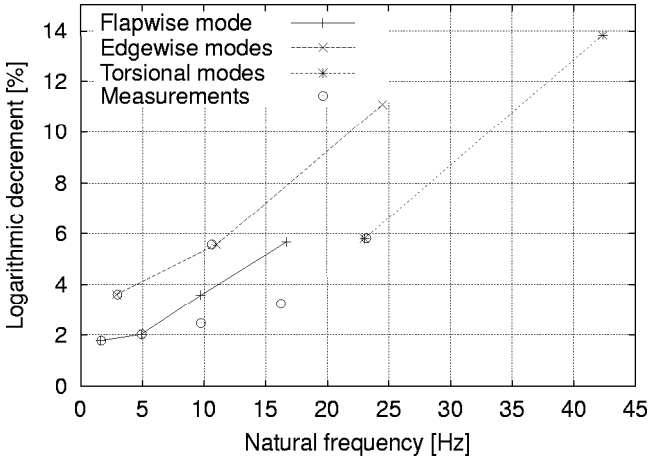

Figure 4. Natural frequencies and logarithmic decrements for the lower modes of the LM 19.1 blade computed using a HawC finite beam element model with 27 nodes. For comparison the measured frequencies and decrements from Figure 1 are also plotted.

damping of this motion becomes more important. The fact that these two different damping mechanisms are governed by a single coefficient may explain why the model cannot capture the damping–frequency curve of flapwise modes.

A possible solution to the problem is an expansion of the suggested model, where *two* coefficients are used to individually define the stiffness proportional damping of translational and rotational motion related to bending. However it is not clear if this solution can be based on the same physical concept of strain–rates dependent damping used in the present model.

4 Conclusion

A viscous damping model for the Timoshenko beam element is suggested. Its purpose is to enable physical modeling of the anisotropic damping of modern wind turbine blades. These blades are often designed with distinct modal damping characteristics of the three principle shapes of vibration: Flapwise bending, edgewise bending, and torsion.

The model is presented by an element damping matrix for a prismatic Timoshenko beam element. The element damping matrix consists of two parts: A part setting the level of damping, and another part describing the frequency dependency of the damping. The first part is a diagonal matrix derived from the diagonals of the element mass and stiffness matrices. The derivation of the second part is based on the physical concept that the frequency dependency of material damping is cause by internal stress-strain hysteresis. Strains due to bending and torsion of the element are proportional to the corresponding moments of inertia, and the second part is therefore derived from the element stiffness matrix.

There are three damping coefficients for each part of the element damping matrix, which enables that the three principle shapes of vibration can be modeled with individual damping–frequency relationships. It might be possible to make universal estimations of these six damping parameters from material tests with simple beam structures. However, for the modeling of a blade it is traditionally preferred to calibrate of the parameters in each case. A procedure for this calibration is presented. It is based on fitting the modal damping obtained from a finite element model of the particular blade (using the damped Timoshenko beam element with the six parameters) to its measured/assumed modal damping characteristics. An example of such calibration shows that the suggested damping model can capture the modal damping of the LM 19.1 blade, except for its higher flapwise modes. It is unknown if this example represents a general insufficiency of the model because damping measurements including the higher modes are not available for other blades. Future developments of the model could include additional damping parameters to handle the higher flapwise modes.

References

[1] R. W. CLOUGH AND J. PENZIEN, *Dynamics of Structures*, McGraw-Hill, Inc., 2nd ed., 1993.

[2] G. COWPER, *The shear coefficient in timoshenko's beam theory*, Journal of Applied Mechanics, (1966), pp. 335–340.

[3] G. LARSEN, M. H. HANSEN, A. BAUMGART, S. M. PETERSEN, AND I. CARLÉN, *Modal analysis of LM 19 blade*, tech. rep., Risø, 2001. (to appear).

[4] J. PETERSEN, *Kinematically Nonlinear Finite Element Model of a Horizontal Axis Wind Turbine*, PhD thesis, Risø National Laboratory, DK-4000 Roskilde, Denmark, 1990.

[5] J. T. PETERSEN, *The aeroelastic code hawc – model and comparisons*, in State of the Art of Aeroelastic Codes for Wing Turbine Calculations, B. M. Pedersen, ed., vol. Annex XI, Lyngby, April 1996, International Energy Agency, Technical University of Denmark, pp. 129–135.

[6] H. ZIEGLER, *Principles of Structural Stability*, Birkhäuser Verlag, 2nd ed., 1977.

A Timoshenko beam element

This appendix contains a brief description of the degrees of freedom for the Timoshenko beam element, and the element mass and stiffness matrices for the prismatic element used in HawC. They are reproduced from the PhD-thesis by Jrgen Thirstrup Petersen [4] where he introduces the HawC model. The purpose of the appendix is only to show the degrees of freedom (DOFs) of the element, and the structure of the element mass and stiffness matrices, see [4] for details.

Concepts and notations

With the Timoshenko beam element it is possible to describe three dimensional motion of a beam structure. Figure 5 shows the six DOFs for each end-node of the element that are used to describe bending about its two primary axes, torsion, and elongation. If the element has a symmetrical cross-section the *shear center*, *elastic center*, and *center of gravity* coincide. In this case, bending motion of any end-node about the x-axis involves only the DOFs $u_{y,i}$ and $\theta_{x,i}$, and bending about the x-axis involves only the DOFs $u_{x,i}$ and $\theta_{y,i}$. Torsion is described by the DOF $\theta_{z,i}$, and longitudinal motion is described by $u_{z,i}$. Note that in a HawC finite element model of a wind turbine blade, the beam elements are oriented with the x-axis closest to the direction of edgewise bending, and the y-axis closest to the flapwise direction.

For asymmetric cross-sections where mass, shear and elastic center do not coincide, there is a coupling between bending and torsion. This effect is included in the derived element matrices [4] listed in the following. Table 1 contains a list of notations for a prismatic Timoshenko beam element.

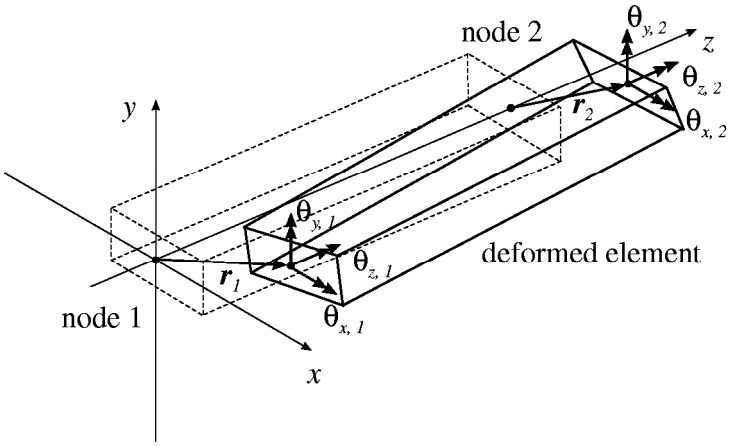

Figure 5. Degrees of freedom for the Timoshenko beam element. The displacement vectors $\mathbf{r}_1 = \{u_{x,1}, u_{y,1}, u_{z,1}\}^T$ *and* $\mathbf{r}_2 = \{u_{x,2}, u_{y,2}, u_{z,2}\}^T$ *describe translations of the end-nodes of the element.*

Parameter	Description
m	Mass per unitlength
ℓ	Length for the element
A	Area of the cross-section
I_x, I_y	Moments of inertia of the cross-section about the x- and y- principle bending axis
E	Modulus of elasticity
I_z	Torsional moment of inertia (for a circular cross-section equal to the polar moment of inertia)
G	Modulus of elasticity in shear
k_x, k_y	Form factors for shear related to forces in x- and y-directions (see [2])
e_{s1}, e_{s2}	x- and y-coordinates for the shear center in element coordinates with origin at the elastic center
r_x, r_y	y- and x-coordinates for the center of mass in element coordinates with origin at the elastic center
r_{Ix}, r_{Iy}	Radii of inertia about the x- and y-axes of the element coordinate system (thus radii of inertia about the center of mass are $\sqrt{r_{Ix}^2 - r_y^2}$ and $\sqrt{r_{Iy}^2 - r_x^2}$)
η_x	$EI_x/(k_y GA\ell^2)$
η_y	$EI_y/(k_x GA\ell^2)$
ϱ_x	$1/(1+12\eta_x)$
ϱ_y	$1/(1+12\eta_y)$
α_x	$(1+3\eta_x)\varrho_x$
α_y	$(1+3\eta_y)\varrho_y$
β_x	$(1-6\eta_x)\varrho_x$
β_y	$(1-6\eta_y)\varrho_y$

Table 1. List of parameters for the Timoshenko beam element.

Element mass matrix

The symmetric element mass matrix can be written on the form:

$$\mathbf{M}_{\text{element}} = \begin{bmatrix} \mathbf{M}_{11} & \mathbf{M}_{12} \\ \mathbf{M}_{12}^T & \mathbf{M}_{22} \end{bmatrix} \tag{A.13}$$

where the 6×6 submatrices are

$$\mathbf{M}_{11} = \begin{bmatrix} m_{1\,1} & 0 & m_{1\,3} & 0 & m_{1\,5} & m_{1\,6} \\ \cdots & m_{2\,2} & m_{2\,3} & m_{2\,4} & 0 & m_{2\,6} \\ \cdots & \cdots & m_{3\,3} & m_{3\,4} & m_{3\,5} & m_{3\,6} \\ \cdots & sym- & \cdots & m_{4\,4} & 0 & m_{4\,6} \\ \cdots & \cdots & metric & \cdots & m_{5\,5} & m_{5\,6} \\ \cdots & \cdots & \cdots & \cdots & \cdots & m_{6\,6} \end{bmatrix}$$

$$\mathbf{M}_{12} = \begin{bmatrix} m_{1\,7} & 0 & m_{1\,3} & 0 & m_{1\,11} & m_{1\,12} \\ 0 & m_{2\,8} & m_{2\,3} & m_{2\,10} & 0 & m_{2\,12} \\ -m_{1\,3} & -m_{2\,3} & m_{3\,9} & m_{3\,10} & m_{3\,11} & -m_{3\,6} \\ 0 & -m_{2\,10} & m_{3\,10} & m_{4\,10} & 0 & m_{4\,12} \\ -m_{1\,11} & 0 & m_{3\,11} & 0 & m_{5\,11} & m_{5\,12} \\ m_{1\,12} & m_{2\,12} & m_{3\,6} & -m_{4\,12} & -m_{5\,12} & m_{6\,12} \end{bmatrix}$$

$$\mathbf{M}_{22} = \begin{bmatrix} m_{1\,1} & 0 & -m_{1\,3} & 0 & -m_{1\,5} & m_{1\,6} \\ \cdots & m_{2\,2} & -m_{2\,3} & -m_{2\,4} & 0 & m_{2\,6} \\ \cdots & \cdots & m_{3\,3} & m_{3\,4} & m_{3\,5} & -m_{3\,6} \\ \cdots & sym- & \cdots & m_{4\,4} & 0 & -m_{4\,6} \\ \cdots & \cdots & metric & \cdots & m_{5\,5} & -m_{5\,6} \\ \cdots & \cdots & \cdots & \cdots & \cdots & m_{6\,6} \end{bmatrix} \tag{A.14}$$

The elements of the first row of the complete 12×12 element matrix are given by

$$\begin{aligned}
m_{1\,1} &= M\varrho_y^2 \left[\left(48\eta_y^2 + \frac{42}{5}\eta_y + \frac{13}{35} \right) + \frac{6}{5} \left(\frac{r_{Iy}}{\ell} \right)^2 \right] \\
m_{1\,3} &= \frac{1}{2} M \varrho_y \frac{r_y}{\ell} \\
m_{1\,5} &= M\ell\varrho_y^2 \left[\left(6\eta_y^2 + \frac{11}{10}\eta_y + \frac{11}{210} \right) - \left(6\eta_y - \frac{1}{10} \right) \left(\frac{r_{Iy}}{\ell} \right)^2 \right] \\
m_{1\,6} &= -Me_{s2}\varrho_y^2 \left[\left(48\eta_y^2 + \frac{42}{5}\eta_y + \frac{13}{35} \right) + \frac{6}{5} \left(\frac{r_{Iy}}{\ell} \right)^2 \right] \\
&\quad - M\varrho_y \left(r_x - e_{s2} \right) \left[4\eta_y + \frac{7}{20} \right] \\
m_{1\,7} &= M\varrho_y^2 \left[24\eta_y^2 + \frac{18}{5}\eta_y + \frac{9}{70} - \frac{6}{5} \left(\frac{r_{Iy}}{\ell} \right)^2 \right] \\
m_{1\,11} &= -M\ell\varrho_y^2 \left[6\eta_y^2 + \frac{9}{10}\eta_y + \frac{13}{420} + \left(6\eta_y - \frac{1}{10} \right) \left(\frac{r_{Iy}}{\ell} \right)^2 \right] \\
m_{1\,12} &= -Me_{s2}\varrho_y^2 \left[24\eta_y^2 + \frac{18}{5}\eta_y + \frac{9}{70} - \frac{6}{5} \left(\frac{r_{Iy}}{\ell} \right)^2 \right] \\
&\quad - M\varrho_y \left(r_x - e_{s2} \right) \left[2\eta_y + \frac{3}{20} \right]
\end{aligned}$$

the second row

$$
\begin{aligned}
m_{2\,2} &= M\varrho_x^2\left[\left(48\eta_x^2+\frac{42}{5}\eta_x+\frac{13}{35}\right)+\frac{6}{5}\left(\frac{r_{Ix}}{\ell}\right)^2\right]\\
m_{2\,3} &= \frac{1}{2}M\varrho_x\frac{r_x}{\ell}\\
m_{2\,4} &= -M\ell\varrho_x^2\left[\left(6\eta_x^2+\frac{11}{10}\eta_x+\frac{11}{210}\right)-\left(6\eta_x-\frac{1}{10}\right)\left(\frac{r_{Ix}}{\ell}\right)^2\right]\\
m_{2\,6} &= Me_{s1}\varrho_x^2\left[\left(48\eta_x^2+\frac{42}{5}\eta_x+\frac{13}{35}\right)+\frac{6}{5}\left(\frac{r_{Ix}}{\ell}\right)^2\right]\\
&\quad + M\varrho_x\left(r_y-e_{s1}\right)\left[4\eta_x+\frac{7}{20}\right]\\
m_{2\,8} &= M\varrho_x^2\left[24\eta_x^2+\frac{18}{5}\eta_x+\frac{9}{70}-\frac{6}{5}\left(\frac{r_{Ix}}{\ell}\right)^2\right]\\
m_{2\,10} &= M\ell\varrho_x^2\left[6\eta_x^2+\frac{9}{10}\eta_x+\frac{13}{420}+\left(6\eta_x-\frac{1}{10}\right)\left(\frac{r_{Ix}}{\ell}\right)^2\right]\\
m_{2\,12} &= Me_{s1}\varrho_x^2\left[24\eta_x^2+\frac{18}{5}\eta_x+\frac{9}{70}-\frac{6}{5}\left(\frac{r_{Ix}}{\ell}\right)^2\right]\\
&\quad + M\varrho_x\left(r_y-e_{s1}\right)\left[2\eta_x+\frac{3}{20}\right]
\end{aligned}
$$

the third row

$$
\begin{aligned}
m_{3\,3} &= \frac{1}{3}M\\
m_{3\,4} &= M\varrho_x r_x\left[4\eta_x+\frac{1}{12}\right]\\
m_{3\,5} &= -M\varrho_y r_y\left[4\eta_y+\frac{1}{12}\right]\\
m_{3\,6} &= \frac{1}{2}M\left[\frac{e_{s1}\varrho_x r_x-e_{s2}\varrho_y r_y}{\ell}\right]\\
m_{3\,9} &= \frac{1}{6}M\\
m_{3\,10} &= M\varrho_x r_x\left[2\eta_x-\frac{1}{12}\right]\\
m_{3\,11} &= -M\varrho_y r_y\left[2\eta_y-\frac{1}{12}\right]
\end{aligned}
$$

the fourth row

$$
\begin{aligned}
m_{4\,4} &= M\ell^2\varrho_x^2\left[\frac{6}{5}\eta_x^2+\frac{1}{5}\eta_x+\frac{1}{105}+\left(48\eta_x^2+2\eta_x+\frac{2}{15}\right)\left(\frac{r_{Ix}}{\ell}\right)^2\right]\\
m_{4\,6} &= -M\ell e_{s1}\varrho_x^2\left[6\eta_x^2+\frac{11}{10}\eta_x+\frac{11}{210}-\left(6\eta_x-\frac{1}{10}\right)\left(\frac{r_{Ix}}{\ell}\right)^2\right]\\
&\quad - M\ell\varrho_x\left(r_y-e_{s1}\right)\left[\frac{1}{2}\eta_x+\frac{1}{20}\right]\\
m_{4\,10} &= -M\ell^2\varrho_x^2\left[\frac{6}{5}\eta_x^2+\frac{1}{5}\eta_x+\frac{1}{140}+\left(-24\eta_x^2+2\eta_x+\frac{1}{30}\right)\left(\frac{r_{Ix}}{\ell}\right)^2\right]\\
m_{4\,12} &= -M\ell e_{s1}\varrho_x^2\left[6\eta_x^2+\frac{9}{10}\eta_x+\frac{13}{420}+\left(6\eta_x-\frac{1}{10}\right)\left(\frac{r_{Ix}}{\ell}\right)^2\right]\\
&\quad - M\ell\varrho_x\left(r_y-e_{s1}\right)\left[\frac{1}{2}\eta_x+\frac{1}{30}\right]
\end{aligned}
$$

the fifth row

$$
\begin{aligned}
m_{5\,5} &= M\ell^2\varrho_y^2\left[\frac{6}{5}\eta_y^2+\frac{1}{5}\eta_y+\frac{1}{105}+\left(48\eta_y^2+2\eta_y+\frac{2}{15}\right)\left(\frac{r_{Iy}}{\ell}\right)^2\right]\\
m_{5\,6} &= -M\ell e_{s2}\varrho_y^2\left[6\eta_y^2+\frac{11}{10}\eta_y+\frac{11}{210}-\left(6\eta_y-\frac{1}{10}\right)\left(\frac{r_{Iy}}{\ell}\right)^2\right]\\
&\quad - M\ell\varrho_y\left(r_x-e_{s2}\right)\left[\frac{1}{2}\eta_y+\frac{1}{20}\right]\\
m_{5\,11} &= -M\ell^2\varrho_y^2\left[\frac{6}{5}\eta_y^2+\frac{1}{5}\eta_y+\frac{1}{140}+\left(-24\eta_y^2+2\eta_y+\frac{1}{30}\right)\left(\frac{r_{Iy}}{\ell}\right)^2\right]\\
m_{5\,12} &= -M\ell e_{s2}\varrho_y^2\left[6\eta_y^2+\frac{9}{10}\eta_y+\frac{13}{420}+\left(6\eta_y-\frac{1}{10}\right)\left(\frac{r_{Iy}}{\ell}\right)^2\right]\\
&\quad - M\ell\varrho_y\left(r_x-e_{s2}\right)\left[\frac{1}{2}\eta_y+\frac{1}{30}\right]
\end{aligned}
$$

and the sixth row

$$
\begin{aligned}
m_{6\,6} &= Me_{s1}^2\varrho_x^2\left[48\eta_x^2+\frac{42}{5}\eta_x+\frac{13}{35}+\frac{6}{5}\left(\frac{r_{Ix}}{\ell}\right)^2\right] \\
&\quad + Me_{s2}^2\varrho_y^2\left[48\eta_y^2+\frac{42}{5}\eta_y+\frac{13}{35}+\frac{6}{5}\left(\frac{r_{Iy}}{\ell}\right)^2\right] \\
&\quad + Me_{s1}\varrho_x\left(r_y-e_{s1}\right)\left[8\eta_x+\frac{7}{10}\right] \\
&\quad + Me_{s2}\varrho_y\left(r_x-e_{s2}\right)\left[8\eta_y+\frac{7}{10}\right] \\
&\quad + \frac{1}{3}M\left(e_{s1}^2+e_{s2}^2+r_{Ix}^2+r_{Iy}^2-2e_{s1}r_y-2e_{s2}r_x\right) \\
m_{6\,12} &= Me_{s1}^2\varrho_x^2\left[24\eta_x^2+\frac{18}{5}\eta_x+\frac{9}{70}-\frac{6}{5}\left(\frac{r_{Ix}}{\ell}\right)^2\right] \\
&\quad + Me_{s2}^2\varrho_y^2\left[24\eta_y^2+\frac{18}{5}\eta_y+\frac{9}{70}-\frac{6}{5}\left(\frac{r_{Iy}}{\ell}\right)^2\right] \\
&\quad + Me_{s1}\varrho_x\left(r_y-e_{s1}\right)\left[4\eta_x+\frac{3}{10}\right] \\
&\quad + Me_{s2}\varrho_y\left(r_x-e_{s2}\right)\left[4\eta_y+\frac{3}{10}\right] \\
&\quad + \frac{1}{6}M\left(e_{s1}^2+e_{s2}^2+r_{Ix}^2+r_{Iy}^2-2e_{s1}r_y-2e_{s2}r_x\right)
\end{aligned}
$$

where $M \equiv m\ell$ is the total mass of the element.

Element stiffness matrix

The symmetric element stiffness matrix can be written on the form:

$$
\mathbf{K} = \begin{bmatrix} \mathbf{K}_{11} & \mathbf{K}_{12} \\ \mathbf{K}_{12}^T & \mathbf{K}_{22} \end{bmatrix} \tag{A.15}
$$

where the 6×6 submatrices are

$$
\begin{aligned}
\mathbf{K}_{11} &= \begin{bmatrix}
k_{1\,1} & 0 & 0 & 0 & k_{1\,5} & k_{1\,6} \\
\cdots & k_{2\,2} & 0 & k_{2\,4} & 0 & k_{2\,6} \\
\cdots & \cdots & k_{3\,3} & 0 & 0 & 0 \\
\cdots & sym- & \cdots & k_{4\,4} & 0 & k_{4\,6} \\
\cdots & \cdots & metric & \cdots & k_{5\,5} & k_{5\,6} \\
\cdots & \cdots & \cdots & \cdots & \cdots & k_{6\,6}
\end{bmatrix} \\
\mathbf{K}_{12} &= \begin{bmatrix}
-k_{1\,1} & 0 & 0 & 0 & k_{1\,5} & -k_{1\,6} \\
0 & -k_{2\,2} & 0 & k_{2\,4} & 0 & -k_{2\,6} \\
0 & 0 & -k_{3\,3} & 0 & 0 & 0 \\
0 & -k_{2\,4} & 0 & k_{4\,9} & 0 & -k_{4\,6} \\
-k_{1\,5} & 0 & 0 & 0 & k_{5\,10} & -k_{5\,6} \\
-k_{1\,6} & -k_{2\,6} & 0 & k_{4\,6} & k_{5\,6} & -k_{6\,6}
\end{bmatrix} \\
\mathbf{K}_{22} &= \begin{bmatrix}
k_{1\,1} & 0 & 0 & 0 & -k_{1\,5} & k_{1\,6} \\
\cdots & k_{2\,2} & 0 & -k_{2\,4} & 0 & k_{2\,6} \\
\cdots & \cdots & k_{3\,3} & 0 & 0 & 0 \\
\cdots & sym- & \cdots & k_{4\,4} & 0 & -k_{4\,6} \\
\cdots & \cdots & metric & \cdots & k_{5\,5} & -k_{5\,6} \\
\cdots & \cdots & \cdots & \cdots & \cdots & k_{6\,6}
\end{bmatrix}
\end{aligned} \tag{A.16}
$$

The elements of the first row of the complete 12×12 element matrix are given by

$$k_{1\,1} = 12\frac{EI_y}{\ell^3}\varrho_y\ , \quad k_{1\,5} = 6\frac{EI_y}{\ell^2}\varrho_y\ , \quad k_{1\,6} = -12\frac{EI_y e_{s2}}{\ell^3}\varrho_y$$

the second row

$$k_{2\,2} = 12\frac{EI_x}{\ell^3}\varrho_x\ , \quad k_{2\,4} = -6\frac{EI_x}{\ell^2}\varrho_x\ , \quad k_{2\,6} = 12\frac{EI_x e_{s1}}{\ell^3}\varrho_x$$

the third row

$$k_{3\,3} = \frac{AE}{\ell}$$

the fourth row

$$k_{4\,4} = 4\frac{EI_x}{\ell}\alpha_x\ , \quad k_{4\,6} = -6\frac{EI_x e_{s1}}{\ell^2}\varrho_x\ , \quad k_{4\,9} = 2\frac{EI_x}{\ell}\beta_x$$

the fifth row

$$k_{5\,5} = 4\frac{EI_y}{\ell}\alpha_y\ , \quad k_{5\,6} = -6\frac{EI_y e_{s2}}{\ell^2}\varrho_y\ , \quad k_{5\,10} = 2\frac{EI_y}{\ell}\beta_y$$

and the sixth row

$$k_{6\,6} = \frac{GI_z}{\ell} + 12\frac{E\left(I_x e_{s1}^2\varrho_x + I_y e_{s2}^2\varrho_y\right)}{\ell^3}$$

B Calibration of parameters

This appendix deals with the calibration of the six damping parameters in the suggested damping model. The idea is to compute these parameter from the condition that the logarithmic decrement for the lower modes of the modeled structure must have certain values. The procedure for this computation is described in five steps.

Step 1 – equations of motion

Set-up the finite element model of the structure by deriving the mass, damping, and stiffness matrices. The damping parameters are still unknown thus the equations of motion for free vibrations described by that model can be written as

$$\mathbf{M}\,\ddot{\mathbf{x}} + \mathbf{C}(\mathbf{p})\,\dot{\mathbf{x}} + \mathbf{K}\,\mathbf{x} = 0 \tag{B.17}$$

where $\mathbf{p} = \{\eta_r^x, \eta_r^y, \eta_r^t, \eta_s^x, \eta_s^y, \eta_s^t\}^T$ is a vector containing the damping parameters, the damping matrix $\mathbf{C}(\mathbf{p})$ is a function of $\mathbf{p}$, and $\mathbf{x}$ is a vector containing the N degrees of freedom (translations and rotations in the nodes).

Step 2 – compute undamped modal properties

To set-up the conditions for calibrating the damping parameters, the natural frequencies and mode shapes for the undamped structure are needed. These are computed from the eigenvalue problem obtained by substitution of $\mathbf{x} = \mathbf{u}_j e^{i\omega_j t}$ into the equations of motion (B.17) without the damping term:

$$\left(-\omega_j^2 \mathbf{M} + \mathbf{K}\right) \mathbf{u}_j = 0 \tag{B.18}$$

where ω_j are the undamped natural frequencies, and $\mathbf{u}_j$ are the undamped mode shapes, or undamped eigenvectors. These eigenvectors are orthogonal with respect to the mass and stiffness matrices. After normalization of the eigenvectors this orthogonality condition can be written as

$$\begin{aligned} \mathbf{u}_i^T\,\mathbf{M}\,\mathbf{u}_j &= \begin{cases} 1 & \text{for } i = j \\ 0 & \text{for } i \neq j \end{cases} \\ \mathbf{u}_i^T\,\mathbf{K}\,\mathbf{u}_j &= \begin{cases} \omega_j^2 & \text{for } i = j \\ 0 & \text{for } i \neq j \end{cases} \end{aligned} \tag{B.19}$$

which is used in the following step.

Step 3 – conditions for calibration

The conditions for calibrating the damping parameters $\mathbf{p}$ are based on the assumption that the level of structural damping is low. It can thereby be assumed that adding of damping does not significantly change the natural frequencies and mode shapes of the structure. Hence the eigenvalues of the damped eigenvalue problem are assumed to be $\lambda_j = \alpha_j + i\omega_j$, where ω_j are the undamped frequencies given by (B.18), and α_j are the modal damping factors obtained from the logarithmic decrements (cf. equation (4)) which the structure is assumed to have. Furthermore, the mode shapes of the damped structure is assumed to be given by the undamped eigenvectors $\mathbf{u}_j$. The error due to these assumptions can be quantified by computing the residuals weighted by the eigenvectors:

$$\mathbf{u}_i^T \left((\alpha_j + i\omega_j)^2\,\mathbf{M} + (\alpha_j + i\omega_j)\,\mathbf{C}(\mathbf{p}) + \mathbf{K} \right) \mathbf{u}_j \approx 0 \quad i,j = 1,\ldots,N \tag{B.20}$$

where the only unknowns are the damping parameters $\mathbf{p}$.

Using that ω_j and $\mathbf{u}_j$ are defined by (B.18), and the orthogonality conditions (B.19), the weighted residuals can be rewritten as

$$\alpha_j\left(\alpha_j + i2\omega_j\right) + \left(\alpha_j + i\omega_j\right)\mathbf{u}_i^T\mathbf{C}(\mathbf{p})\,\mathbf{u}_j \approx 0 \quad i,j = 1,\ldots,N \tag{B.21}$$

which all have a real and an imaginary part. It is noted that these two parts of each residual can not both be satisfied. However because of low damping $\omega_j >> \alpha_j$, the real part is neglected and only the imaginary part is considered. After use of orthogonality the imaginary part of the weighted residuals can be written as

$$\mathbf{u}_i^T\mathbf{C}(\mathbf{p})\,\mathbf{u}_j \;\approx\; \begin{cases} -2\alpha_j & \text{for } i = j \\ 0 & \text{for } i \neq j \end{cases} \qquad i,j = 1,\ldots,N \tag{B.22}$$

These residuals only depend on $\mathbf{p}$ and therefore gives the conditions for computing the damping parameters. The weighted residuals for $i \neq j$ describes that there should be no modal coupling of the undamped modes due to the damping forces. This is the case for a Rayleigh damping model, but for the suggested model these residuals may not vanish (this does not mean that the suggested model includes inter-modal damping coupling, the eigenvectors of the damped system are orthogonal with respect to the symmetric damping matrix).

Step 4 – compute damping parameters

The computation of the damping parameters is based on equation (B.22) for $i = j$. Because there are six unknown parameters, at least six equations are needed to compute $\mathbf{p}$, thus the logarithmic decrements of only six modes need to be specified. The choice of modes is free, however it is a good practice to at least include the two lowest modes of the three vibration shapes: Two transversal bending, and torsion. The reason is that the six damping parameters are related in pairs to these three vibration shapes (cf. Section 3).

Assume that the decrements for $N_d \geq 6$ modes have been specified, and that the chosen modes are given by a list m_j where $j = 1,\ldots,N_d$. The least square method to minimize the residuals for these modes then yields the equation

$$\mathbf{A}^T\mathbf{A}\;\mathbf{p} = -2\mathbf{A}^T\mathbf{d} \tag{B.23}$$

where $\mathbf{A}$ is a $N_d \times 6$ matrix containing the derivatives:

$$A_{m_j n} = \frac{d}{dp_n}\left(\mathbf{u}_{m_j}^T\mathbf{C}(\mathbf{p})\,\mathbf{u}_{m_j}\right) \qquad j = 1,\ldots,N_d \text{ and } n = 1,\ldots,6 \tag{B.24}$$

and $\mathbf{d} = \{\alpha_{m_1},\ldots,\alpha_{m_{N_d}}\}^T$ is a vector containing the modal damping factors for the chosen modes. The damping parameters that minimize the residuals for these modes can now be computed as the solution of equation (B.23). The validity of the result is discussed in the fifth and last step.

Step 5 – validate damping parameters

For some choices of modes and corresponding logarithmic decrements it can occur that one or more of the computed damping parameters are negative, whereby the definiteness of the damping matrix becomes unknown. Such solution is discarded because the damping matrix must be positive definite for the modeled damping forces to be purely dissipative (cf. Section 3).

The cases where the suggested damping model leads to a non-physical damping characteristics, an adjustment of the logarithmic decrements may overcome the problem. However, if the decrements have all been measured, the model must be reconsidered for the particular structure.

Bibliographic Data Sheet **Risø–R–1267(EN)**

Title and author(s)

Anisotropic damping of Timoshenko beam elements

Morten Hartvig Hansen

ISBN
87–550–2881–0; 87–550–2883–7 (Internet)

ISSN
0106–2840

Dept. or group
Aeroelastic Design
Wind Energy Department

Date
May 29, 2001

Groups own reg. number(s)

Project/contract No.
ENS 1363/00-0007
ENK6-CT2000-00320

Pages	Tables	Illustrations	References
26	1	5	6

Abstract (Max. 2000 char.)

This report contains a description of a structural damping model for Timoshenko beam elements used in the aeroelastic code HawC developed at Ris for modeling wind turbines. The model has been developed to enable modeling of turbine blades which often have different damping characteristics for *flapwise*, *edgewise* and *torsional* vibrations. The structural damping forces acting on the beam element are modeled by viscous damping described by an element damping matrix. The composition of this matrix is based on the element mass and stiffness matrices. It is shown how the coefficients for the mass and stiffness contributions can be calibrated to give the desired modal damping in the complete model of a blade.

Descriptors INIS/EDB

MECHANICAL VIBRATIONS; DAMPING; FINITE ELEMENT METHOD; MATHEMATICAL MODELS; STRUCTURAL BEAMS; TURBINE BLADES; WIND TURBINES

Available on request from:
Information Service Department, Risø National Laboratory
(Afdelingen for Informationsservice, Forskningscenter Risø)
P.O. Box 49, DK–4000 Roskilde, Denmark
Phone (+45) 46 77 46 77, ext. 4004/4005 · Fax (+45) 46 77 4013